Photothermal Characterization of Electrochemical Etching Processed *n*-Type Porous Silicon

A. Calderón, J. J. Alvarado-Gil, and Yu. G. Gurevich
Departimento dee Fisica, CINVESTAV-IPN, A.P. 14-740, 07000 México, Districto Federal, Mexico

A. Cruz-Orea, and I. Delgadillo
Programa Multidisciplinario de Ciencias Aplicadas y Tecnologia Avanzada, CINVESTAV-IPN, A.P. 14-740, 07000 México, Districto Federal, Mexico

H. Vargas
Laboratorio de Ciencias Fisicas, Universidade Estadual do Norte Fluminense, Av. Alberto Lamego 2000, 28015-620 Campos dos Goytacazes, Rio de Janeiro, Brasil

L. C. M. Miranda
Laboratorio de Sensores e Materials, Instituto Nacional de Pesquisas Espaciais, 12243-010 São José dos Campos, São Paulo, Brasil

(Received 19 July 1996)

The room temperature thermal diffusivity evolution of electrochemically formed porous silicon as a function of the etching time is investigated. The measurements were carried out using the open-cell photoacoustic technique. The experimental data were analyzed using a composite two-layer model. The results obtained strongly support the existing studies, indicating the presence of a high percentage of SiO_2 in the composition of porous silicon material. [S0031-9007(97)04884-9]

PACS numbers: 44.30.+v, 61.43.Gt, 81.05.Cy, 81.05.Rm

Since the discovery of its room-temperature visible luminescence [1–5], porous silicon (PS) has become a subject of considerable interest, especially for its promising use as an optoelectronic device [6,7]. There are several methods [8–11] for fabricating PS from crystalline silicon wafers. The electrochemical etching [1,8] is, however, the most extensively used so far. The morphology of the resulting porous layer is strongly dependent upon the fabrication controlling parameters such as electrolyte composition, current density, etching time, etc., as well as on the type of substrate used.

In general, an electrochemically formed *n*-type PS layer consists essentially of a double-layer system on top of the silicon substrate [1,12]. The outermost thin layer, known as the microporous layer, is typically 10–15 μm thick and is responsible for the observed photoluminescence. Except for very small etching times, the inner layer adjacent to the crystalline substrate, designated as the macroporous layer, consists of a parallel array of air-embedded free-standing *n*-PS columns.

Despite the large body of literature that already exists on PS [13,14], so far there has been no reported detailed investigation of the thermophysical properties of this important system. In this Letter we apply the modern photothermal techniques to the evaluation of the thermal properties of electrochemically formed *n*-PS.

The samples used in our experiments were prepared by electrochemical etching on (100) oriented, nondegenerated, *n*-type (2.1×10^{18} cm^{-3}) crystalline silicon. The samples had a thickness of roughly 300 μm and an electrical resistivity of 1–5 Ω cm. The electrochemical etching was carried out following the procedure outlined in Ref. [12]. The crystalline samples, with an appropriate Pt network electrode attached to them, were immersed in a 150 ml Becker filled with HF. A current density of 40 mA/cm^2 was then applied to the samples using a HP-model 6206B dc power supply operating between 5–10 V. During the etching period the samples were always kept under the irradiation of a 250 W infrared lamp positioned roughly 20 cm away from the etching bath. By controlling the etching time, ranging from 10 to 83 min, we could fabricate samples with different macroporous thicknesses.

In Fig. 1 we show the side view optical micrograph of a typical *n*-PS sample, produced with 60 min etching time. The three distinct regions mentioned above, namely, the microporous and macroporous layers on top of the crystalline substrate, are clearly seen in this picture.

The room-temperature thermal diffusivity measurements were carried out using the photoacoustic (PA) technique. Of the several techniques [15] used for measuring the thermal diffusivity, we resorted to the so-called "open cell" technique described in Refs. [16] and [17]. It consists of mounting the sample directly onto a cylindrical electret microphone and using the front air chamber of the microphone itself as the usual gas chamber of conventional photoacoustics, as indicated in Fig. 2. The measurements were carried out using a 20 mW He-Ne laser whose monochromatic light beam is modulated using a variable speed mechanical chopper (SRS model 540) and focused onto the sample. The microphone output voltage is measured using a lock-in amplifier (SRS model 850).

 0031-9007/97/79(25)/5022(4)$10.00

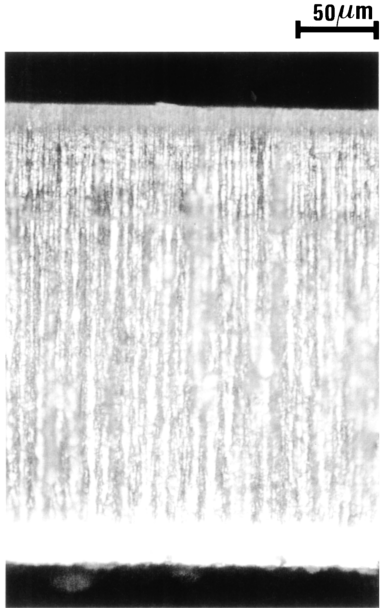

FIG. 1. Optical microscope side view of cleaved *n*-PS sample, etched during 60 min.

All the data acquisition was microcomputer controlled. The thermal diffusivity is obtained from the modulation frequency dependence of the detected PA signal, as discussed in detail in Refs. [16] and [17]. That is, using the thermal diffusion model for the PA effect, the measurement signal S in the modulation frequency range, where the sample is thermally thick, may be written as [16]

$$S = (A/f)\exp(-a\sqrt{f}), \tag{1}$$

where $a = l(\pi/\alpha)^{1/2}$ is the sample thermal diffusion coefficient, and A is constant related to the air thermal properties, light intensity, etc. Here, l is the sample thickness and α is its thermal diffusivity.

It thus follows that the value of α is readily obtained from the signal amplitude modulation frequency scanning data fitting to Eq. (1). In Fig. 3 we show the results we obtained for the thermal diffusivity of our *n*-PS samples as a function of the relative thickness (etching time) of the macroporous layer. The thickness, as well as the volume fraction of the solid matter within the macroporous layer, was measured using optical microscopy. That is, for each sample prepared with a given etching time, we have estimated both the thickness and the average solid volume fraction of the macroporous layer using optical microscope images at normal and side views.

To understand the observed dependence of α on the macroporous layer thickness, we assume that our sample may be viewed as the layered system schematically shown in Fig. 4. That is, the *n*-PS sample consists of a macroporous layer and the remaining crystalline silicon labeled 1 and 2, respectively, in Fig. 4. The macroporous layer, on the other hand, is assumed to consist of an air-embedded array of parallel Si columns. The air and Si columns within the macroporous layer are labeled by 3 and 4, respectively. Here, it should be mentioned that we are implicitly neglecting the contribution of the thin ($\sim$12 μm thick) microporous layer to the *n*-PS thermal properties. We shall return to this point later. In terms of this series two-layer system, the thermal diffusivity for the heat flow perpendicular to the sample surface may be written as [16–19]

$$\alpha = \frac{1}{\dfrac{x^2}{\alpha_1} + \dfrac{(1-x)^2}{\alpha_2} + x(l-x)\left[\dfrac{\lambda_{12}}{\alpha_1} + \dfrac{1}{\lambda_{12}\alpha_2}\right]}, \tag{2}$$

where $x = l_1/l$ and $\lambda_{12} = k_1/k_2$. Here l_1 is the mean thickness of region 1, l is the total sample thickness, and k_1 and α_1 denote the thermal conductivity and diffusivity of the region i. The thermal properties of medium 1 are, in turn, expressed in terms of the corresponding properties of their constituent media, 3 and 4. For the parallel system, consisting of Si columns embedded in air, the effective thermal conductivity k_1 and heat capacity $\rho_1 c_1$

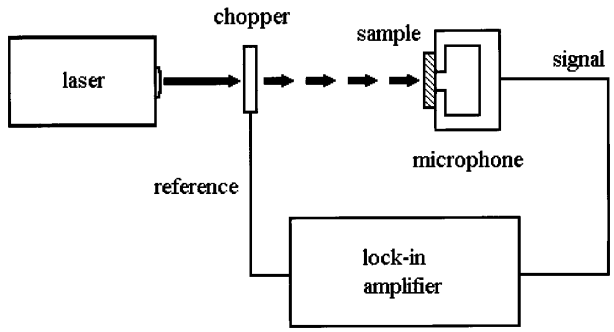

FIG. 2. Schematic of the experimental arrangement for the open-cell photoacoustic measurement of the thermal diffusivity.

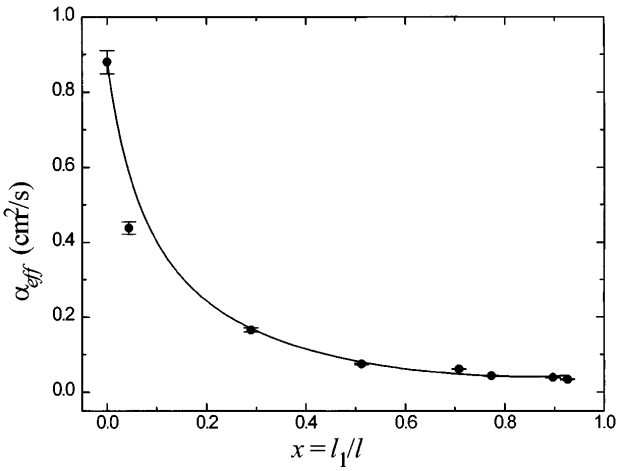

FIG. 3. Thermal diffusivity as a function of the relative macroporous layer thickness for the *n*-PS samples, as determined by the photoacoustic measurements. The solid curve shows the best fitting of the effective thermal diffusivity expressed as a function of x (see text).

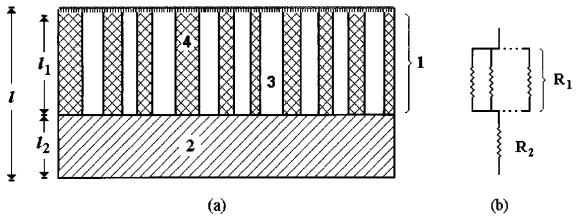

FIG. 4. (a) Schematic representation of the two-layer system. The top dashed layer represents the microporous layer. (b) Electrical analog of the two-layer system in which R_2 denotes the substrate thermal resistance and R_1 denotes the equivalent thermal resistance of the parallel array of columnar material of the macroporous layer.

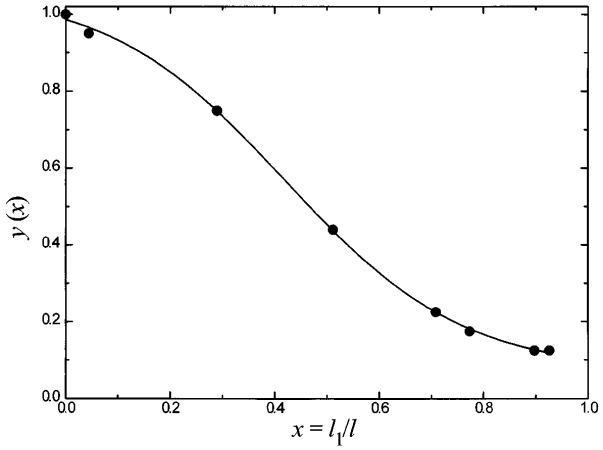

FIG. 5. Volume fraction of the solid material with the macroporous layer y versus its relative thickness x as obtained from the optical microscopy image analyses. The solid curve represents the data best fit to the logistic curve given by Eq. (6) of the text.

can be written as

$$k_1 = k_2 + (k_4 - k_3)y\,, \tag{3}$$

$$\rho_1 c_1 = \rho_3 c_3 + (\rho_4 c_4 - \rho_3 c_3)y\,. \tag{4}$$

where y denotes the volume fraction of the solid material within medium 1. Equations (3) and (4) lead to the following expression for $\alpha_1 = k_1/\rho_1 c_1$:

$$\alpha_1 = \alpha_3 \frac{1 + y(\lambda - 1)}{1 + y(\sigma - 1)}\,. \tag{5}$$

where $\lambda = k_4/k_3$ and $\sigma = \rho_4 c_4/\rho_3 c_3$. Equations (2), (3), and (5), completely define the effective thermal diffusivity of our n-PS system. The only unknown parameters in the resulting expression for α are the thermal properties of the Si columns in the n-PS samples. The other intervening parameters are the thermal properties of air, crystalline silicon, and the volume fraction y of the Si columns in medium 1. Thus, provided the morphological parameter y is known, the thermal properties of the columnar material in region 1 is readily obtained from the fitting of the resulting expression for α to the experimental values of Fig. 3.

The relative macroporous layer thickness x and the volume fraction of the solid material y are, indeed, intimate related to each other, and strongly dependent upon the n-PS formation mechanism [1,2]. As previously mentioned, for each sample investigated, we have evaluated the volume fraction y using the normal and side view optical microscope images. In Fig. 5, we show the resulting data for y as a function of the relative thickness of the macroporous layer of our n-PS samples. The data was best fitted to an S-shape curve represented by a logistic function, namely

$$y(x) = 1 - \Delta y \exp\left(\frac{x - x_0}{\Delta x}\right) \Big/ \left[1 + \exp\left(\frac{x - x_0}{\Delta x}\right)\right]. \tag{6}$$

Here Δy represents the excursion to reach the saturation value, taking place during an interval Δx, and x_0 is the thickness at which the fractional change $(y - y_0)/\Delta y$ reaches halfway to the saturation excursion. The result obtained from the data fitting of y to Eq. (6), leaving Δy, x_0, and Δx adjustable parameters, is shown in Fig. 5 by the solid curve. The values obtained for the fitting parameters were $\Delta y = 0.994 \pm 0.024$, $x_0 = 0.421 \pm 0.011$, and $\Delta x = 0.170 \pm 0.013$.

Using the above expression for the volume fraction, as well as values of the thermal properties of Si ($k_2 = 1.48$ W/cm K, $\alpha_2 = 0.88$ cm^2/s) and air ($k_3 = 0.00026$ W/cm K, $\alpha_3 = 0.21$ cm^2/s) [20], and carrying out the best fit of the α to Eq. (2), yielded the following values for the thermal properties of the columnar material: $\alpha_4 = 0.053 \pm 0.0035$ cm^2/s and $k_4 = 0.130 \pm 0.006$ W/cm K [these values are quite close to those of SiO_2 ($a = 0.045$–0.061 cm^2/s and $k = 0.104$ W/cm K)] [20] which suggests that a high percentage of this material is, indeed, present in the composition of the n-PS columns [4,21]. The results of this best fit is shown in Fig. 3 by the solid curve. This somewhat unexpected result for the values of the thermal properties of the columnar material in the macroporous layer close to those of SiO_2 deserves further investigation. Probably, repeating the same measurements after a sample dip in HF may give us an answer as to whether SiO_2 is really the material contributing to these values of the thermal properties, or is there another cause.

As a final test of the appropriateness of neglecting the contribution of the thin microporous layer to the thermal diffusivity measurements, which is implicit in the above model, we have performed the same PA measurements with two randomly chosen samples for which the microporous layers have been removed. The removal of the microporous layer was done by careful mechanical polishing. The results we obtained for the thermal diffusivity, within our 5% experimental error, were essentially the same. Physically, the reason for this is that the thermal

diffusion time, $\tau = l^2/\alpha$, within the microporous layer is negligible as compared to the remaining, two-layer system of the *n*-PS sample. Assuming that the thermal diffusivity of the microporous layer (~ 12 μm thick) lies between that of Si and SiO_2, the thermal diffusion time in this layer ranges from 1.6 to 32 μs. In contrast, for a typical microporous layer ($x = 0.5$), the thermal diffusion time in the two-layer system is of the order of 9 ms. That is, for the heat diffusion, the thin microporous layer may be viewed as thermally transparent for heat transmission.

In conclusion, it should be mentioned that the methodology present here is not restricted to the case of *n*-PS sample and can be applied equally to the thermal characterization of morphologically similar materials.

This work was partially supported by CONACyT, México. The authors thank the valuable collaboration of A. Dudiño-Martínez, R. Fragoso Soriano, P. Rodríguez Fragoso, M. Guerrero Gruz, and E. Ayala Maycotte for their technical assistance at different stages of this paper.

[1] L. T. Canham, Appl. Phys. Lett. **57**, 1046 (1990).
[2] V. Lehmann and U. Gosele, Appl. Phys. Lett. **58**, 856 (1991).
[3] P. C. Searson, J. M. Macaulay, and F. M. Ross, Appl. Phys. Lett. **72**, 253 (1992).
[4] R. E. Hummel, A. Morrone, M. Ludwig, and S.-S. Chang, Appl. Phys. Lett. **63**, 2771 (1993).
[5] D. Rüter, T. Kunze, and W. Bauhofer, Appl. Phys. Lett. **64**, 3006 (1994).
[6] N. M. Kalkhoran, F. Namavar, and H. P. Maruska, Appl. Phys. Lett. **63**, 2661 (1993).
[7] D. J. Lockwood, Solid State Commun. **92**, 101 (1994).
[8] M. I. J. Beale, J. D. Benjamin, M. J. Uren, N. G. Chew, and A. G. Cullis, J. Crystal Growth **73**, 622 (1985).
[9] R. E. Hummel and S.-S. Chang, Appl. Phys. Lett. **61**, 1965 (1992).
[10] Y. Kanernitsu, H. Uto, Y. Masumoto, and Y. Yaeda, Appl. Phys. Lett. **61**, 2187 (1992).
[11] Y. Maeda, N. Tsukamoto, Y. Yazawa, Y. Kanemitsu, and Y. Masumoto, Appl. Phys. Lett. **59**, 3168 (1991).
[12] V. Lehman and H. Föll, J. Electrochem. Soc. **137**, 653 (1990).
[13] Y. Kanemitsu, Phys. Rep. **263**, 1–92 (1995).
[14] G. C. John and V. A. Singh, Phys. Rep. **263**, 93 (1995).
[15] H. Vargas and L. C. M. Miranda, Phys. Rep. **161**, 43 (1988).
[16] A. M. Mansanares, A. C. Bento, H. Vargas, N. F. Leite, and L. C. M. Miranda, Phys. Rev. B **42**, 4477 (1990).
[17] E. Marín, J. L. Pichardo, A. Cruz-Orea, P. Díaz, G. Torres-Delgado, I. Delgadillo, J. J. Alvarado-Gil, J. G. Mendoza-Alvarez, and H. Vargas, J. Phys. D **29**, 981 (1996).
[18] G. González de la Cruz and Yu. G. Gurevich, Phys. Rev. B **51**, 2188 (1995).
[19] A. Cruz-Orea, I. Delgadillo, H. Vargas, A. Gudiño-Martínez, E. Marín, C. Vázquez-López, A. Calderón, and J. J. Alvarado-Gil, J. Appl. Phys. **79**, 8951 (1996).
[20] Y. S. Touloukian, R. W. Powell, C. Y. Ho, and M. C. Nicolaou, *Thermophysical Properties of Matter* (Plenum, New York, 1970).
[21] J. M. Perez, J. Villalobos, P. McNeill, J. Prasad, R. Cheek, J. Kelber, J. P. Estrera, P. D. Stevens, and R. Glosser, Appl. Phys. Lett. **61**, 563 (1992).